nature structural & molecular biology

Structure of a topoisomerase II–DNA–nucleotide complex reveals a new control mechanism for ATPase activity

Bryan H Schmidt[1], Neil Osheroff[2,3] & James M Berger[1]

Type IIA topoisomerases control DNA supercoiling and disentangle chromosomes through a complex ATP-dependent strand-passage mechanism. Although a general framework exists for type IIA topoisomerase function, the architecture of the full-length enzyme has remained undefined. Here we present the structure of a fully catalytic *Saccharomyces cerevisiae* topoisomerase II homodimer complexed with DNA and a nonhydrolyzable ATP analog. The enzyme adopts a domain-swapped configuration wherein the ATPase domain of one protomer sits atop the nucleolytic region of its partner subunit. This organization produces an unexpected interaction between bound DNA and a conformational transducing element in the ATPase domain, which we show is critical for both DNA-stimulated ATP hydrolysis and global topoisomerase activity. Our data indicate that the ATPase domains pivot about each other to ensure unidirectional strand passage and that this state senses bound DNA to promote ATP turnover and enzyme reset.

Elaborate multiprotein assemblies serve myriad vital cellular roles throughout biology[1]. Typically composed of a diverse suite of distinct types of catalytic folds and scaffolding elements, these so-called 'molecular machines' collate and coordinate distinct functional activities as a means to link and streamline complex biochemical transactions. Although the roles and actions of different classes of molecular machines are both diverse and varied, many such systems exhibit highly articulated movements that are driven by ligand-binding and ligand-exchange events. The conversion of nucleoside triphosphates into directed motion and force is a particularly prevalent theme among these systems. How the various components composing a given machine are organized into higher-order structures and how such elements coordinate their respective catalytic functions are outstanding questions in biology.

Type II topoisomerases are archetypal nucleic acid–remodeling enzymes[2]. Using ATP as a cofactor, different type II topoisomerase family members can variously add or remove DNA supercoils and either form or unlink DNA tangles and knots. These topological rearrangements rely on a multistage mechanism that involves the controlled association and dissociation of distinct subunit-dimerization interfaces, or 'gates', which help guide the physical movement of one DNA duplex through another[3–7]. The type IIA topoisomerases, found predominantly in bacteria and eukaryotes, possess three such interfaces, termed the N gate, DNA gate and C gate (**Fig. 1a**)[2]. In the type IIA reaction cycle, one double-stranded DNA (termed the G segment) is bound and cleaved by the enzyme, while a second duplex (the 'T segment') is transported through the break[8]. G-segment breakage is catalyzed by a pair of symmetrically related tyrosines[9,10], in conjunction with a Mg^{2+} ion–binding topoisomerase-primase (Toprim) fold[11], to form a transient covalent topoisomerase–DNA cleavage complex. Strand passage is coordinated by defined ATPase domains[12–14], which use ATP binding and hydrolysis to promote T-segment capture, stimulate G-segment cleavage and coordinate successive opening and closing of the gates[3,8,15,16].

Despite extensive study, a number of fundamental questions persist regarding both the configuration of the type IIA topoisomerase holoenzyme and the coordination of the enzyme catalytic cycle by ATP. Although crystal structures of isolated ATPase and DNA-binding-and-cleavage regions of these enzymes have been reported (for example, refs. 5–7 and 17), how these elements are juxtaposed with respect to each other remains unknown. Mechanistically, how DNA binding stimulates ATP turnover[18–20] and why ATP hydrolysis is sequential rather than synchronous (at least in yeast topoisomerase II)[21] likewise have been difficult to explain at a structural or biochemical level. Because type II topoisomerases are members of the broader pantheon of GHKL-family ATPases[22], a group that includes MutL-family DNA-repair proteins and Hsp90-type chaperones, answers to these questions are likely to broadly resonate across diverse biochemical systems.

To define the global architecture of a type IIA topoisomerase holoenzyme, we determined what is, to our knowledge, the first crystal structure of a fully functional construct of *S. cerevisiae* topo II trapped in a covalent cleavage complex with a G-segment DNA and the nonhydrolyzable ATP analog AMPPNP. The structure not only definitively establishes the relative juxtaposition between the ATPase regions and the DNA-binding-and-cleavage core but also reveals two unexpected higher-order organizational features: a double domain-swapping event between ATPase subunits, which forms a topological

[1]Department of Molecular and Cell Biology, University of California, Berkeley, Berkeley, California, USA. [2]Department of Biochemistry, Vanderbilt University School of Medicine, Nashville, Tennessee, USA. [3]Department of Medicine (Hematology/Oncology), Vanderbilt University School of Medicine, Nashville, Tennessee, USA. Correspondence should be addressed to J.M.B. (jmberger@berkeley.edu).

Received 24 May; accepted 23 August; published online 30 September 2012; doi:10.1038/nsmb.2388

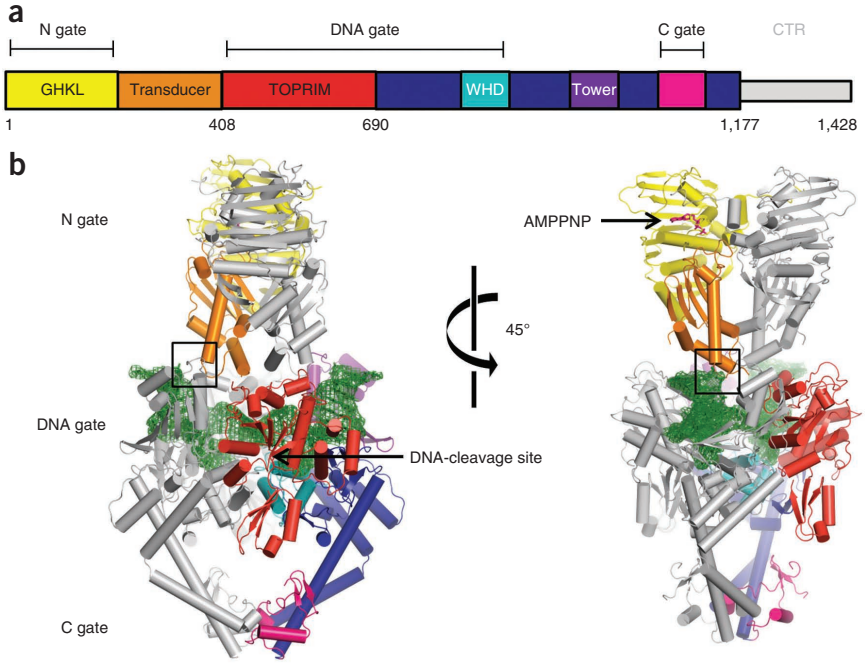

Figure 1 Structure of topo II bound to DNA and AMPPNP. (**a**) Domain arrangement of type IIA topoisomerases. Functional regions are colored and labeled. CTR, C-terminal region. (**b**) Model of the ternary complex. One topo II protomer is shaded gray, the other colored as in **a**. Green indicates $2F_o - F_c$ density (1.5σ contour) shown around the DNA (green sticks).

barrier to strand passage, and an interaction between the highly bent G segment and a lysine-rich loop in the ATPase domain. Biochemical studies validate the ATPase-DNA interaction, showing not only that it is critical for activity in both yeast and human topo IIα but also that it serves as a communication relay that couples DNA binding to the stimulation of ATP turnover. Together, these findings point to the existence of new and hitherto unsuspected intermediate states in the type IIA topoisomerase strand-passage cycle and highlight how discrete functional activities can be coordinated across long distances in a large macromolecular system.

RESULTS

Structure of a functional topo II–DNA–AMPPNP complex

One impediment to imaging the ATPase and DNA-binding-and-cleavage elements of type IIA topoisomerases in conjunction with each other derives from the large size and dynamic nature of these enzymes. In particular, the three dimerization interfaces can each exist in an associated or dissociated state to give rise to significant conformational variability within a population. To capture a minimally flexible state, we first used a nicked DNA oligonucleotide containing a single phosphorothiolate site as a suicide substrate to trap a covalent cleavage complex with a functional *S. cerevisiae* topo II construct comprising amino acids 1–1,177 (**Fig. 1a**, **Supplementary Fig. 1** and Online Methods). Prior studies of covalent type IIA topoisomerase–DNA complexes, which used either this type of substrate or a drug-inhibited state, have found that formation of the phosphotyrosyl linkage coincides with closure of the DNA gate and C gate of the enzyme[23–29]. We then added the nonhydrolyzable ATP analog AMPPNP, which is known to lock the ATPase gate into its dimerized, clamped form[3,5], as a means to promote association of all three interfaces. Crystals grown from this complex belonged to the space group $P2_12_12_1$ and permitted the collection of diffraction data to 4.4-Å resolution. Subsequent rounds of molecular replacement (MR) using single protomers of the isolated yeast topo II cleavage core and ATPase domain produced a solution that recapitulated a full topo II dimer in the asymmetric unit. Because of the moderate resolution of the data, side chain positions were generally left in the position found in the original search model during refinement (Online Methods). Despite these relatively modest adjustments, the final structure was readily refined to an R_{work}/R_{free} of 24.0/27.7% with good stereochemistry (**Fig. 1b**, **Table 1** and Online Methods). Notably, the dimeric conformations of the ATPase domain and DNA-binding-and-cleavage core in the holoenzyme match those seen for the two regions observed in isolation, which indicated that these structural states correspond to commonly populated intermediates in the topo II reaction cycle (**Supplementary Fig. 2**).

Topo II ATPase elements swap domains to contact DNA

Organizational models for full-length type IIA topoisomerases have, in general, suggested that the ATPase domains arch over the G-segment binding surface[6,30,31]. The actual orientation between the two regions has been the subject of speculation, however, both because the two

Table 1 Data collection and refinement statistics

	Topo II–DNA–AMPPNP
Data collection	
Space group	$P2_12_12_1$
Cell dimensions	
a, *b*, *c* (Å)	169.14, 169.88, 169.21
α, β, γ (°)	90, 90, 90
Resolution (Å)	50–4.4 (4.57–4.41)
R_{sym}	7.6 (70.3)
$I / \sigma I$	15.5 (2.0)
Completeness (%)	91.7 (92.9)
Redundancy	4.3 (4.2)
Refinement	
Resolution (Å)	50–4.4
No. reflections	28,660
R_{work} / R_{free}	23.9 / 27.5
No. atoms	
Protein	18,050
DNA	2,118
AMPPNP	62
Mg^{2+}	2
B factors	
Protein	238.5
DNA	278.7
AMPPNP	233.4
Mg^{2+}	115.1
R.m.s. deviations	
Bond lengths (Å)	0.004
Bond angles (°)	0.842

Values in parentheses are for highest-resolution shell.

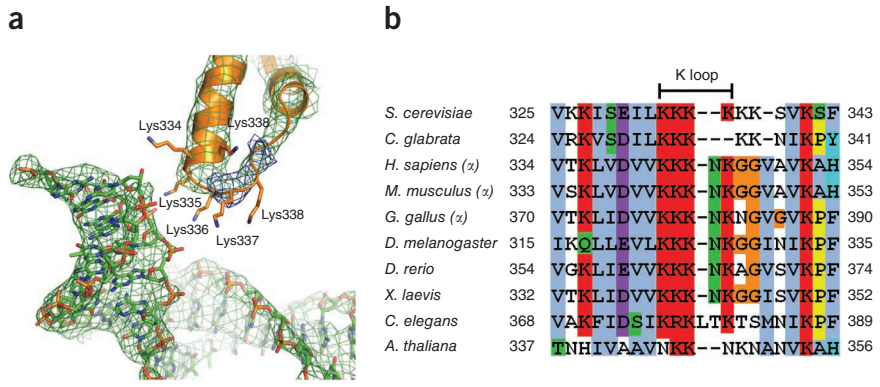

Figure 2 The topo II ATPase domain appears to engage bound DNA. (**a**) Close-up view of the K-loop interaction with DNA. View corresponds to the boxed region in **Figure 1b**. DNA is surrounded by $2F_o - F_c$ density contoured to 1.5σ. The K loop is surrounded by $2F_o - F_c$ density contoured to 1.0σ (green) as well as original $F_o - F_c$ density from the initial MR solution, contoured to 2.5σ (blue). The original search model had a gap spanning residues 335–339. (**b**) Sequence alignment of eukaryotic type IIA topoisomerases. The K-loop lysines are bracketed. The human, mouse and chicken sequences correspond to the α isoforms; topo IIβ isoforms also bear K-loop lysines.

functional elements are connected by a flexible and proteolytically sensitive linker[12–14] and because structures of the isolated ATPase domains have exhibited a crossover, at their extreme C termini, whose relevance has remained uncertain[5,17,32–34]. Our model shows that the ATPase domains do indeed sit atop the site of G-segment association and cleavage but that the central cavity of the ATPase-domain dimer is offset by approximately 45° from the hole that runs between the DNA gate and C gate (**Fig. 1b**). Notably, the juxtaposition of the domains appears to give rise to a domain-swapping event, such that the ATPase region of one protomer contacts the Toprim fold of its associated partner subunit (**Supplementary Fig. 3**).

In addition to domain swapping, the topo II configuration present in the crystal exhibits a second distinctive feature: an apparent contact between the ATPase 'transducer' subdomain and the backbone of the bent G-segment DNA (**Figs. 1** and **2a**). A closer view of this region highlights a loop that emanates from the outer edge of the transducer domain to take up a position proximal to the DNA backbone. The amino acid sequence conservation of this region, hereafter termed the K loop, is somewhat variable among type IIA topoisomerases but retains up to six consecutive lysines, several of which are well conserved among eukaryotic topo II homologs (**Fig. 2b**). In previous higher-resolution structures of the isolated ATPase domains of yeast and human topo IIα, the K loop has been disordered and unmodeled[17,34]. By contrast, the peptide chain is readily visible in electron density for both protomers seen here (**Fig. 2a**). Although the resolution of our structure precludes precise modeling of side chain rotamers, the appearance of electron density for the K-loop main chain suggests that this region becomes ordered upon engaging DNA. Our structure also suggests that there may exist additional contacts between each transducer domain and both the Toprim and 'tower' domains of its symmetry-related protomer; however, the resolution of our data does not permit us to definitively model specific interactions between these elements.

The K loop is important for DNA strand-passage activities

To our knowledge, a functional role for the K loop *per se* has not been established previously. A prior study has shown that deleting a 57-residue area of the transducer region encompassing the K loop eliminates DNA-stimulated ATPase activity[35], but the molecular basis for this effect was not determined. To test whether specific contacts between the K loop and DNA might be important for topo II activity, we replaced various lysines in this stretch of the *S. cerevisiae* enzyme with either alanine or glutamate and examined the ability of the mutant constructs to relax negatively supercoiled DNA. In this assay, purified plasmid was incubated with a fixed starting level of ATP and increasing concentrations of topo II, after which the reaction products were analyzed by agarose gel electrophoresis (Online Methods). The appearance of discrete DNA topoisomers that migrate more slowly than the starting supercoiled substrate is a hallmark of the DNA relaxation reaction catalyzed by type II topoisomerases other than DNA gyrase[36].

We initially found that single Lys→Ala mutations at each of the six lysines in this region did not noticeably affect supercoil relaxation (data not shown). However, stronger effects became apparent as individual mutations were combined; a construct bearing a quadruple KKKK→AAAA mutation in the first four amino acids of the K loop displayed approximately one-fourth the level of supercoil relaxation activity (**Fig. 3**). Because any interaction between the K loop and DNA is likely to rely on a significant electrostatic component, we reasoned that introducing negative charges at the most highly conserved lysine positions might more significantly affect topo II activity. We therefore prepared a KKKK→AEEA mutant, in which the two most highly conserved lysines were replaced with glutamates. This mutant exhibits less than 10% of the specific activity of the wild-type enzyme (**Fig. 3a**). Notably, both the AEEA protein and its AAAA counterpart could be expressed and purified under identical conditions as with wild-type topo II and showed no abnormal migration behavior, as assayed by size-exclusion chromatography

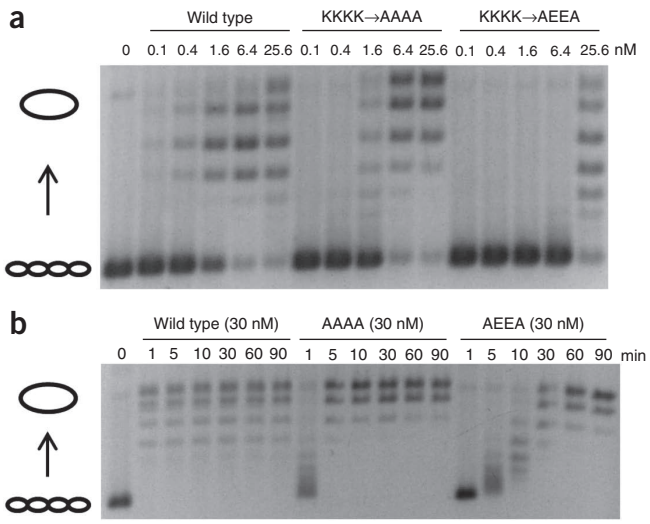

Figure 3 K-loop mutants are deficient at relaxing negatively supercoiled DNA. (**a**) Concentration-dependent relaxation of negatively supercoiled DNA. Supercoiled and relaxed topoisomers are denoted with coiled and open circles, respectively. (**b**) Time course–dependent negative supercoil relaxation. In both sets of reactions, 7.5 nM DNA is present.

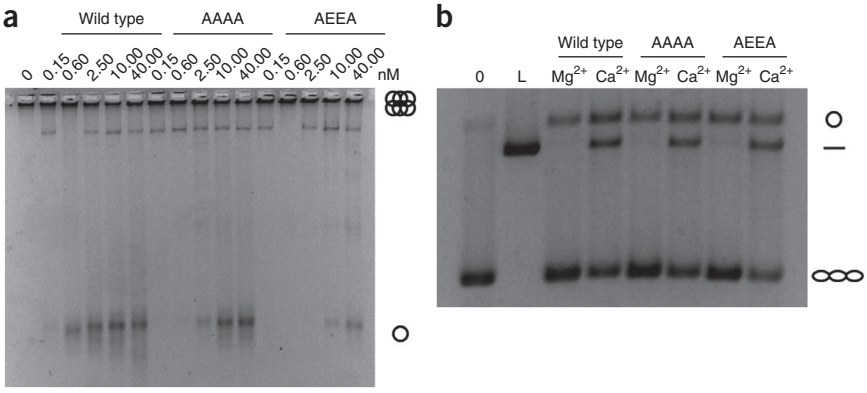

Figure 4 K-loop mutants are defective for decatenation but not for DNA cleavage. (**a**) Decatenation assay. The degree to which the AAAA and AEEA mutants are impaired in decatenation activity follows the trend seen for the relaxation of negatively supercoiled DNA. (**b**) Cleavage assay in the presence of Mg^{2+} or Ca^{2+} ions as shown. 0, negative control, no protein; L, plasmid linearized by BamHI. The wild type and K-loop mutants show similar propensities to cleave DNA in a calcium-dependent manner.

(**Supplementary Fig. 4** and Online Methods), which indicated that the loss of activity displayed by the mutants is not due to folding or assembly defects. The relative distributions of topoisomer populations also differ between the mutant and wild-type proteins, which suggests that K-loop integrity may have a role in enzyme processivity.

S. cerevisiae topo II is unusual among eukaryotic type IIA topoisomerases in that it bears six lysines in its K loop; most other orthologs possess three, including the two that appear universally conserved in eukaryotes (**Fig. 2b**). To determine whether the observed effects of K-loop substitutions on DNA supercoiling could be generalized, we cloned, expressed and purified the KKK→AAA and KKK→EEE triple mutants of human topo IIα. Negative-supercoil relaxation assays were carried out and analyzed for the mutant and wild-type topo IIα proteins as for yeast topo II. The resultant data show that both mutants impede the removal of supercoils, with the Lys→Glu charge substitutions again producing a more severe defect in activity compared to alanine substitutions (**Supplementary Fig. 5a,b**). Thus, the K loop appears to play a part in strand passage across different topo II orthologs.

To more precisely define the action of the K loop, we examined DNA decatenation by yeast topo II and the K-loop mutants. Decatenation can be assessed by incubating purified enzyme with kinetoplast DNA (kDNA) and ATP and then resolving the products by agarose gel electrophoresis. kDNA normally comprises a large catenated network of mini-circles that cannot enter a standard agarose gel; however, the unlinking action of a type II topoisomerase produces individual mini-circles that migrate freely into the matrix[37]. Using this assay, we found that the AAAA and AEEA mutants display reduced levels of activity comparable to those seen during supercoil relaxation (**Fig. 4a**). These results show that the role of the K loop is not restricted to the type of DNA substrate encountered by topo II but is instead necessary to support overall strand passage.

Because defects in strand passage could arise from an impaired ability to cleave DNA, we next set out to investigate the strand-scission properties of the enzyme. Cleavage was examined by an initial incubation of yeast topo II with negatively supercoiled plasmid DNA in the presence of AMPPNP and either Mg^{2+} or Ca^{2+} ions, followed by rapid denaturation of the complex with SDS and resolution of the products on an agarose gel. Ca^{2+} is known to stimulate cleavage over background levels of cutting[38] to form a species that comigrates with linearized vector. Notably, both the AAAA and AEEA mutants produce similar amounts of linear DNA as does the wild-type enzyme (**Fig. 4b**). These results support the position that topo II K-loop mutants are not generally compromised by a folding or assembly defect and that the integrity of this region is necessary to support the strand-passage reaction following G-segment binding and cleavage.

The K loop couples DNA binding to ATPase activity

Loss of supercoil relaxation and decatenation activities can, in principle, arise from a deficiency in one of any number of steps in the type IIA topoisomerase catalytic cycle. Having established that DNA cleavage appears unperturbed in our K-loop mutants, we next examined the ATPase activity of the enzyme. The transducer subdomain on which the K loop resides is known to have a key role in ATP hydrolysis, providing an invariant amino acid (Lys367 in yeast topo II) that plugs into the GHKL nucleotide-binding pocket. Although the K loop sits ~50 Å away from this active site residue, residing instead on the outer edge of the ATPase region (**Fig. 1b**), we reasoned that it might nonetheless indirectly influence nucleotide turnover at a distance. Using an established coupled assay to report on ATPase function[39,40], we first assessed the basal ATPase rates between the wild-type, AAAA and AEEA topo II constructs. The overall profiles of all three proteins are similar (**Fig. 5a**), with the AEEA actually exhibiting a slightly greater level of specific activity than the other two enzymes. The V_{max} and K_m values obtained from these curves also are similar (**Supplementary Fig. 5c,d**) and in line with values reported previously for the wild-type yeast enzyme[19]. Hence, the intrinsic ATPase activity of topo II does not appear to be compromised by K-loop alterations, which again indicates that the substitutions do not directly impair the folding or function of the domain.

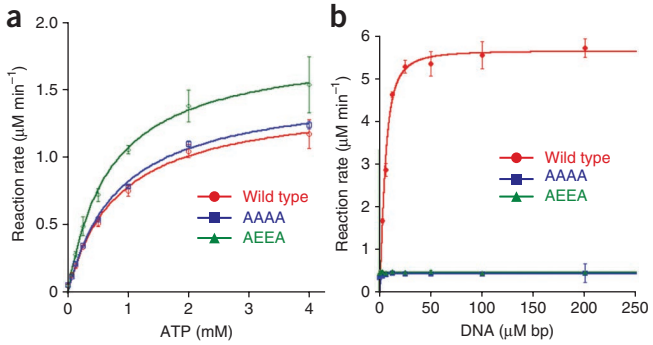

Figure 5 K-loop mutants maintain basal ATPase rates but lose DNA stimulation of ATP hydrolysis. (**a**) Basal ATPase activity. Wild-type and K loop–mutant activities are shown plotted as a function of ATP concentration and fit to a standard Michaelis-Menten kinetic model. Apparent V_{max} values of 1.42 ± 0.06, 1.51 ± 0.06 and 1.82 ± 0.05 μM min^{-1} were calculated for wild type, AAAA and AEEA topo II constructs, respectively. Calculated K_m values were 0.82 ± 0.09, 0.84 ± 0.09 and 0.70 ± 0.05 mM ATP, respectively. (**b**) DNA-stimulated ATPase activity. Wild-type and K loop–mutant activities monitored at a constant starting concentration of ATP and plotted as a function of sheared salmon sperm DNA concentration. Error bars, s.d. from three independent experiments.

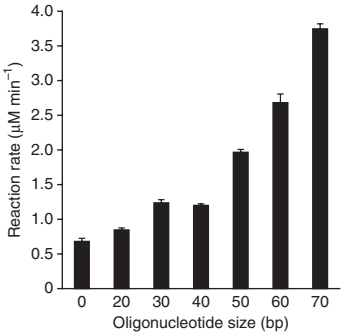

Figure 6 Oligonucleotides stimulate ATP hydrolysis in a length-dependent manner. A 20-mer oligonucleotide fails to stimulate ATP hydrolysis beyond the basal rate. As length increases, ATPase stimulation increases. The molar ratio of DNA:protein is 250:1 for these data, and error bars are s.d. from three independent experiments.

By contrast, the influence of DNA on the ATPase rate of mutant enzymes is striking. It has been well established that DNA stimulates ATP turnover by more than an order of magnitude in most type IIA topoisomerases studied to date[18–20,41]. To assess this effect for our K-loop mutants, we measured ATPase rates at a single starting ATP concentration in the presence of increasing amounts of sheared salmon sperm DNA. The ATPase activity of our wild-type topo II preparations was stimulated ~15-fold in this assay (**Fig. 5b**), a level consistent with prior measurements for this enzyme *in vitro*[19]. By contrast, both the AAAA and AEEA topo II mutants failed to exhibit stimulation upon the addition of DNA (**Fig. 5b**). To ensure that this effect was not limited to the yeast enzyme, we measured whether DNA could stimulate the activity of human topo IIα. Consistent with prior observations[42,43], the degree of enhancement observed for our wild-type topo IIα protein was ~20-fold; however, DNA only doubles the ATPase activity of the two topo IIα K-loop mutants (**Supplementary Fig. 5c**,**d**). Together, these data indicate that the K loop has an unexpected but direct role in coupling DNA binding with ATP turnover and strand passage.

Inspection of our crystal structure shows that the K loop appears to interact with a DNA region that flanks the nucleolytic center and site of DNA bending (**Figs. 1c** and **2a**). If the K loop indeed detects whether DNA is stably associated with the enzyme, then the nature of this contact predicts that sensing should be dependent on the length of the G segment associated with the primary DNA binding and cleavage center: that is, oligonucleotides shorter than 30 base pairs (bp) should not be long enough to reach the K loop and thus should stimulate ATPase rates only minimally, whereas longer oligonucleotides should extend past the ATPase domain and allow contact to occur. To test this assumption, we investigated the role of DNA oligonucleotide length on the stimulation of ATPase rate. A series of oligonucleotides, ranging from 20 to 70 bp and each containing a centered preferred site for topo II binding[44], were individually added to ATPase reactions containing wild-type topo II, and their effects were monitored as a function of turnover rate. Notably, the intact 20-mer substrate was unable to appreciably stimulate ATP turnover, even at a saturating molar ratio (250:1) of DNA to enzyme. By contrast, as the length of the intact oligonucleotides was increased at a constant DNA concentration, the ATPase activity of the enzyme also increased (**Fig. 6** and **Supplementary Fig. 6**). These findings are consistent with the concept that bound G-segment DNA needs to be of a certain length to reach the ATPase domains and their associated K loops.

DISCUSSION

A complete topo II–DNA–nucleotide structure

Despite being generally accepted by the community, the structural organization of a fully functional type IIA topoisomerase has not been definitively established. The work described here fills this gap, resolving the question of how the ATPase domains connect with the rest of the enzyme (**Fig. 1**). The only part of the enzyme missing in our construct is a poorly conserved C-terminal region (residues 1,178–1,428), which contains both phosphorylation and nuclear-localization sites[45,46]. In human topo IIα, this element has a role in stimulating the relaxation of positive supercoils. However, the C-terminal tail is not required for negative-supercoil relaxation, nor are its stimulatory properties retained by its paralog, topo IIβ (ref. 47). Moreover, deletion of the C terminus of *S. cerevisiae* topo II has no effect on DNA strand passage compared to that of the full-length protein *in vitro*[48]. Hence, our structure reflects a minimal type IIA topoisomerase variant that possesses all of the elements necessary to support normal strand-passage activities.

One notable feature of our full-length model—which derives from a complete view of the topo II holoenzyme in the crystal—is that its two major functional parts, the ATPase domains and the DNA-binding-and-cleavage core, adopt dimeric conformational states that are essentially indistinguishable from structures of the same regions in isolation from each other (**Supplementary Fig. 2**)[17,27]. This finding supports the biological relevance of these and other fragment-derived models to our understanding of type IIA topoisomerase mechanism as a whole. In particular, we see that the interior hole formed between the dimerized topo II ATPase domains remains much smaller than that seen for the equivalent regions of bacterial type IIA enzymes (**Supplementary Fig. 2**)[5,17,32–34]. This finding is notable because the size of this feature in topo II would appear to preclude stable binding and trapping of DNA in its nucleotide-bound form. This observation likely accounts for the known inability of yeast topo II to accommodate a T segment before DNA-gate opening[49].

Notably, nearly all dimerized type IIA topoisomerase ATPase domain models visualized to date have displayed an intertwined structure that results from domain-swapping events at both the N and C termini (**Supplementary Fig. 2**)[5,17,32–34]. Although the significance of this doubly wrapped configuration has remained unclear, particularly insofar as the modest contact seen at the extreme C terminus, we note that it is preserved in the DNA- and AMPPNP-bound topo II structure observed here (**Supplementary Fig. 3**). This consistency strongly suggests that the reciprocal exchange of ATPase-domain elements is a universal feature of type IIA topoisomerases that reflects a specific intermediate in the catalytic cycle. Notably, this domain-swapping event leads to the topological segregation of the upper ATPase-domain hole from the G-segment binding surface. Taken together with the small interior hole manifest between the dimerized topo II ATPase domains, these physical features suggest that our model most likely corresponds to a state that follows both nucleotide binding and T-segment transport. Consistent with this proposal, biochemical studies of yeast topo II have shown that AMPPNP can support a single complete round of DNA passage but that the ATPase domains remain dimerized, preventing further rounds of activity[8,50,51].

A direct connection between the ATPase elements and DNA

The coupling between DNA binding and ATP turnover is one of the most enigmatic aspects of type II topoisomerase function, and of many nucleic acid–dependent motors in general. A particularly unexpected feature of the ternary complex imaged here is the appearance of a direct connection between the ATPase 'transducer'

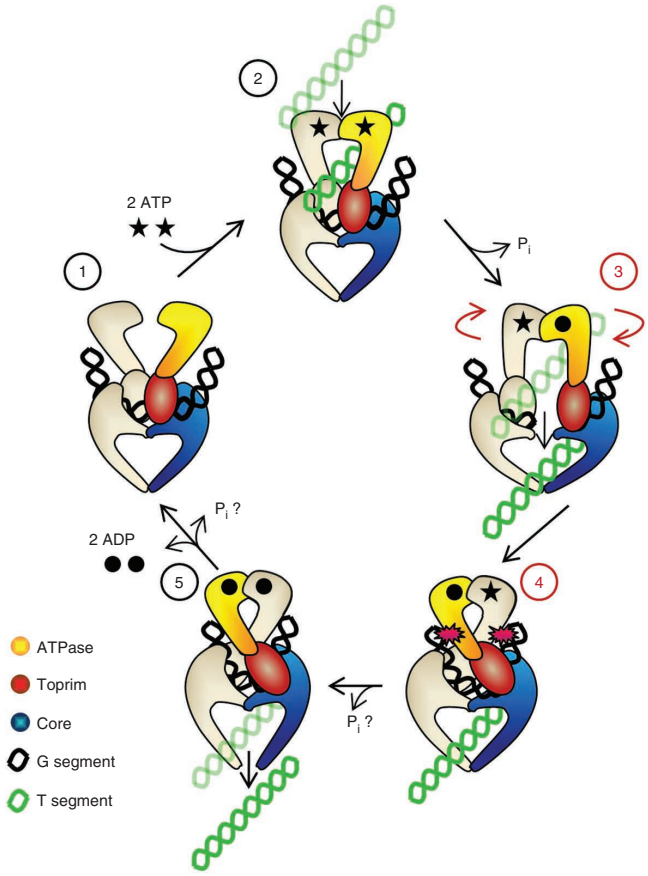

Figure 7 Unexpected complexities in the type IIA topoisomerase catalytic cycle. (1) Homodimer at the beginning of cycle. One monomer is shaded gray and the other is colored as indicated in the key. The enzyme binds and bends a G segment (black). (2) The binding of two ATPs (stars) promotes capture of the T-segment (green). (3) Hydrolysis of one ATP to ADP (circle) leads to G-segment cleavage and T-segment transport through the break. Following strand transport, the ATPase domains swivel about each other to impede backward translocation of the T segment. (4) G-segment ends are brought back together for religation. K-loop contacts are proposed to trigger hydrolysis of the second ATP. (5) T-segment escape, followed by ADP release, resets the enzyme. Steps (3) and (4) are highlighted in red to denote the new findings from this work; as many prokaryotic type IIA topoisomerases appear to lack a K loop (**Supplementary Fig. 8**), interactions between this region and G-segment DNA as shown in (4) may be limited to eukaryotic topo II homologs. The precise point of P_i release following the second hydrolysis step is not known (question marks).

subdomain and the bound G-segment DNA (**Fig. 2**). Site-directed mutagenesis of conserved lysines in this region of both yeast topo II and human topo IIα did not appreciably affect DNA cleavage but did adversely affect both DNA decatenation and supercoil-relaxation activity (**Figs. 3** and **4**; **Supplementary Fig. 5a**,**b**). Moreover, the K-loop mutations resulted in an essentially complete loss of DNA-stimulated ATPase activity without affecting basal ATP turnover rates (**Fig. 5** and **Supplementary Fig. 5c**,**d**). These data indicate that the K-loop–DNA interaction that we observed occurs in solution and that the K loop itself is a hitherto unanticipated control element for coupling DNA binding with nucleotide hydrolysis at a distance. They also establish DNA as a conduit for linking the site of G-segment binding and bending with catalysis by the ATPase centers of the enzyme.

The dependence of DNA length in stimulating ATPase activity further corroborates the K-loop–G-segment interaction (**Fig. 6**). Whereas the stimulatory effect of a 20-mer oligonucleotide substrate on hydrolysis rates is negligible, even when present in vast excess over enzyme, increasing DNA length results in progressively greater activity. Crystal structures have shown that 20-mer duplexes can be bound and cleaved by the G segment–binding core[23,26]; however, these substrates do not extend far enough out of the active site to engage the K loop. Notably, longer oligonucleotide substrates do not approach the stimulatory effect of sheared salmon sperm DNA (**Figs. 5b** and **6**), whose average length is on the order of hundreds of base pairs. This result suggests that although the K-loop–G-segment interaction directly contributes to ATPase stimulation, the interaction by itself is not sufficient to account for the full stimulation by DNA on ATPase rates. As previous work has implicated T-segment binding to the ATPase in the stimulation of ATPase activity[42,52], it is possible that salmon sperm DNA is more stimulatory because it is sufficiently long to serve as both a G and T segment. Alternatively (or in addition), there may exist additional contacts between G-segment DNA and the transducer or GHKL ATPase fold further up the domain, which our structure does not reveal because of the short length (30 bp) of our DNA.

An inspection of the literature provides additional support for the K-loop–DNA contact that we observe. A prior protein footprinting study using *S. cerevisiae* topo II identified five lysines that become protected upon binding DNA[53]. Four of these residues lie in the major DNA-binding groove of the catalytic core and are masked by the associated G segment; however, the fifth lysine was found to reside on the K loop. Although a role for this region was not known at the time of this effort, the authors speculated that protection within this region might have resulted from a conformational change or from direct DNA interactions—the present work indicates that it is both. In a second, more recent investigation, high-throughput mass spectrometry revealed that human topo IIβ is subject to acetylation[54]. Notably, three acetylation sites were discovered, all of which either reside on or are proximal to the K-loop region (Lys365, Lys367 and Lys373 in hTop2β numbering). The biological significance of modifying these residues, if any, is not known but, on the basis of the findings described here, this might serve as a specific means for regulating topo IIβ activity inside the cell.

Complexities in type IIA topoisomerase DNA strand passage

If the structure reported here corresponds to a functional intermediate in the topo II strand-passage cycle, then what might be the purpose of the domain swapping that we observed between ATPase-domain elements? In the current generalized version of the type IIA topoisomerase catalytic cycle, both a G and a T segment must be captured by the enzyme before ATP binding (**Fig. 7**)[3,6,8,30]. Nucleotide association drives dimerization of the ATPase domains, along with cleavage and opening of the G segment and passage of the T segment through the break. During passage, the T-segment DNA is generally considered to transit exclusively from the N-terminal portion of the protein to its C-terminal side[4,16]. Unidirectionality is thermodynamically aided by the consumption of ATP[55]; however, the mechanical motions that enforce one-way movement have been ill defined. The ability of the ATPase domains to wrap around themselves provides one possible solution to this problem, as a crossover of the protein chain would provide a physical impediment to movement of the T segment back through the cleaved G segment once passage has occurred. We note that this scheme would require the dimerized ATPase domains to twist about each other by perhaps as much as 180° before locking into

place against the G segment, following transport (**Fig. 7**). Although this twist seems extreme, an inspection of the ATP-dimerized Hsp90 chaperone, which employs the same family of ATPase fold as topo II, shows that it intertwines around itself to a similar extent (**Supplementary Fig. 7**)[56].

Our structure raises a second unanticipated issue involving the type IIA topoisomerase mechanism, namely why these enzymes might have evolved a contact that allows the ATPase domains to sense the presence of a properly bound and bent G segment *after* strand passage has occurred. One possibility is that this contact affords an extra layer of control to more tightly couple ATP turnover with strand passage. Outside of gyrase, which uses the free energy of ATP to add negative supercoils to DNA[57], the need for ATP in the type IIA topoisomerase reaction has remained uncertain. One model is that ATP serves as a timing element, or 'gatekeeper', that temporarily promotes the formation of a new dimer interface during DNA cleavage to secure the two DNA ends[55]. Because establishment of the nucleolytic center appears to coincide with a very precisely phased DNA bend[23,25,27,28,58], having the ATPase domains touch the G segment could help signal that the passage reaction is complete and that ATP can be hydrolyzed to allow enzyme reset. Consistent with this idea, pre–steady state kinetic studies have shown that the ATPase elements of *S. cerevisiae* topo II fire asynchronously, with one ATP hydrolyzed before or concomitant with strand passage and the other hydrolyzing later, likely after strand passage is complete[21]. These data suggest that the K-loop–DNA interaction that we observed may predominantly affect the second ATPase event (**Fig. 7**). In accord with this reasoning, a human topo IIα heterodimer containing only a single functional ATP-binding site is weakly able to relax DNA supercoils but shows no DNA-stimulated ATPase activity[59]; our model would predict that this mutant enzyme can support only the first ATP turnover step that drives strand passage but not the step required to stimulate enzyme turnover. Similarly, biochemical analyses have indicated that the ATPase activity of *Bacillus subtilis* gyrase, which lacks the K loop, is not asynchronous[60]. Future studies will be needed to test these concepts further.

Concluding remarks

Type IIA topoisomerases are multisubunit DNA-remodeling enzymes that undergo a series of highly articulated movements to physically move one DNA duplex through another. The structural and biochemical studies reported here definitively establish the higher-order structural organization of this class of enzymes and further reveal new architectural linkages that help couple ATP turnover with strand passage. These findings highlight some of the unanticipated and sophisticated complexities that can be employed by molecular machines, particularly those that rely or act on nucleic acids, to coordinate disparate catalytic events in support of essential biochemical transactions.

METHODS

Methods and any associated references are available in the online version of the paper.

Accession codes. Coordinates and structure factors for the structure have been deposited in the Protein Data Bank, with accession code 4GFH.

Note: Supplementary information is available in the online version of the paper.

ACKNOWLEDGMENTS

The authors thank A. Burgin, at Emerald BioStructures, Bainbridge Island, Washington, USA, for synthesizing the phosphorothioamidite reagent, as well as members of the Berger Lab for helpful discussions. This work was supported by a US National Institutes of Health training grant (GM08295 to B.H.S.) and the US National Cancer Institute (CA077373 to J.M.B.) and the US National Institutes of Health (GM33944 to N.O.).

AUTHOR CONTRIBUTIONS

B.H.S., J.M.B. and N.O. designed the experiments. B.H.S. performed all of the experiments. B.H.S. and J.M.B. wrote the paper.

COMPETING FINANCIAL INTERESTS

The authors declare no competing financial interests.

Published online at http://www.nature.com/doifinder/10.1038/nsmb.2388.
Reprints and permissions information is available online at http://www.nature.com/reprints/index.html.

1. Bustamante, C., Cheng, W. & Mejia, Y.X. Revisiting the central dogma one molecule at a time. *Cell* **144**, 480–497 (2011).
2. Schoeffler, A.J. & Berger, J.M. DNA topoisomerases: harnessing and constraining energy to govern chromosome topology. *Q. Rev. Biophys.* **41**, 41–101 (2008).
3. Roca, J. & Wang, J.C. The capture of a DNA double helix by an ATP-dependent protein clamp: a key step in DNA transport by type II DNA topoisomerases. *Cell* **71**, 833–840 (1992).
4. Roca, J., Berger, J.M., Harrison, S.C. & Wang, J.C. DNA transport by a type II topoisomerase: direct evidence for a two-gate mechanism. *Proc. Natl. Acad. Sci. USA* **93**, 4057–4062 (1996).
5. Wigley, D.B., Davies, G.J., Dodson, E.J., Maxwell, A. & Dodson, G. Crystal structure of an N-terminal fragment of the DNA gyrase B protein. *Nature* **351**, 624–629 (1991).
6. Berger, J.M., Gamblin, S.J., Harrison, S.C. & Wang, J.C. Structure and mechanism of DNA topoisomerase II. *Nature* **379**, 225–232 (1996).
7. Morais Cabral, J.H. *et al.* Crystal structure of the breakage-reunion domain of DNA gyrase. *Nature* **388**, 903–906 (1997).
8. Roca, J. & Wang, J.C. DNA transport by a type II DNA topoisomerase: evidence in favor of a two-gate mechanism. *Cell* **77**, 609–616 (1994).
9. Worland, S.T. & Wang, J.C. Inducible overexpression, purification, and active site mapping of DNA topoisomerase II from the yeast *Saccharomyces cerevisiae*. *J. Biol. Chem.* **264**, 4412–4416 (1989).
10. Tse, Y.C., Kirkegaard, K. & Wang, J.C. Covalent bonds between protein and DNA. Formation of phosphotyrosine linkage between certain DNA topoisomerases and DNA. *J. Biol. Chem.* **255**, 5560–5565 (1980).
11. Aravind, L., Leipe, D.D. & Koonin, E.V. Toprim–a conserved catalytic domain in type IA and II topoisomerases, DnaG-type primases, OLD family nucleases and RecR proteins. *Nucleic Acids Res.* **26**, 4205–4213 (1998).
12. Lindsley, J.E. & Wang, J.C. Study of allosteric communication between protomers by immunotagging. *Nature* **361**, 749–750 (1993).
13. Gellert, M., Fisher, L.M. & O'Dea, M.H. DNA gyrase: purification and catalytic properties of a fragment of gyrase B protein. *Proc. Natl. Acad. Sci. USA* **76**, 6289–6293 (1979).
14. Brown, P.O., Peebles, C.L. & Cozzarelli, N.R. A topoisomerase from *Escherichia coli* related to DNA gyrase. *Proc. Natl. Acad. Sci. USA* **76**, 6110–6114 (1979).
15. Williams, N.L. & Maxwell, A. Locking the DNA gate of DNA gyrase: investigating the effects on DNA cleavage and ATP hydrolysis. *Biochemistry* **38**, 14157–14164 (1999).
16. Williams, N.L. & Maxwell, A. Probing the two-gate mechanism of DNA gyrase using cysteine cross-linking. *Biochemistry* **38**, 13502–13511 (1999).
17. Classen, S., Olland, S. & Berger, J.M. Structure of the topoisomerase II ATPase region and its mechanism of inhibition by the chemotherapeutic agent ICRF-187. *Proc. Natl. Acad. Sci. USA* **100**, 10629–10634 (2003).
18. Mizuuchi, K., O'Dea, M.H. & Gellert, M. DNA gyrase: subunit structure and ATPase activity of the purified enzyme. *Proc. Natl. Acad. Sci. USA* **75**, 5960–5963 (1978).
19. Lindsley, J.E. & Wang, J.C. On the coupling between ATP usage and DNA transport by yeast DNA topoisomerase II. *J. Biol. Chem.* **268**, 8096–8104 (1993).
20. Osheroff, N., Shelton, E.R. & Brutlag, D.L. DNA topoisomerase II from *Drosophila melanogaster*. Relaxation of supercoiled DNA. *J. Biol. Chem.* **258**, 9536–9543 (1983).
21. Harkins, T.T., Lewis, T.J. & Lindsley, J.E. Pre-steady-state analysis of ATP hydrolysis by *Saccharomyces cerevisiae* DNA topoisomerase II. 2. Kinetic mechanism for the sequential hydrolysis of two ATP. *Biochemistry* **37**, 7299–7312 (1998).
22. Dutta, R. & Inouye, M. GHKL, an emergent ATPase/kinase superfamily. *Trends Biochem. Sci.* **25**, 24–28 (2000).
23. Laponogov, I. *et al.* Structural basis of gate-DNA breakage and resealing by type II topoisomerases. *PLoS ONE* **5**, e11338 (2010).
24. Laponogov, I. *et al.* Structural insight into the quinolone-DNA cleavage complex of type IIA topoisomerases. *Nat. Struct. Mol. Biol.* **16**, 667–669 (2009).
25. Wohlkonig, A. *et al.* Structural basis of quinolone inhibition of type IIA topoisomerases and target-mediated resistance. *Nat. Struct. Mol. Biol.* **17**, 1152–1153 (2010).
26. Bax, B.D. *et al.* Type IIA topoisomerase inhibition by a new class of antibacterial agents. *Nature* **466**, 935–940 (2010).

27. Schmidt, B.H., Burgin, A.B., Deweese, J.E., Osheroff, N. & Berger, J.M. A novel and unified two-metal mechanism for DNA cleavage by type II and IA topoisomerases. *Nature* **465**, 641–644 (2010).
28. Wu, C.C. *et al.* Structural basis of type II topoisomerase inhibition by the anticancer drug etoposide. *Science* **333**, 459–462 (2011).
29. Wendorff, T.J., Schmidt, B.H., Heslop, P., Austin, C.A. & Berger, J.M. The structure of DNA-bound human topoisomerase II alpha: conformational mechanisms for coordinating inter-subunit interactions with DNA cleavage. *J. Mol. Biol.* published online, doi:10.1016/j.jmb.2012.07.014 (25 July 2012).
30. Kampranis, S.C., Bates, A.D. & Maxwell, A. A model for the mechanism of strand passage by DNA gyrase. *Proc. Natl. Acad. Sci. USA* **96**, 8414–8419 (1999).
31. Schultz, P., Olland, S., Oudet, P. & Hancock, R. Structure and conformational changes of DNA topoisomerase II visualized by electron microscopy. *Proc. Natl. Acad. Sci. USA* **93**, 5936–5940 (1996).
32. Lamour, V., Hoermann, L., Jeltsch, J.M., Oudet, P. & Moras, D. An open conformation of the *Thermus thermophilus* gyrase B ATP-binding domain. *J. Biol. Chem.* **277**, 18947–18953 (2002).
33. Brino, L. *et al.* Dimerization of *Escherichia coli* DNA-gyrase B provides a structural mechanism for activating the ATPase catalytic center. *J. Biol. Chem.* **275**, 9468–9475 (2000).
34. Wei, H., Ruthenburg, A.J., Bechis, S.K. & Verdine, G.L. Nucleotide-dependent domain movement in the ATPase domain of a human type IIA DNA topoisomerase. *J. Biol. Chem.* **280**, 37041–37047 (2005).
35. Bjergbaek, L. *et al.* Communication between the ATPase and cleavage/religation domains of human topoisomerase IIα. *J. Biol. Chem.* **275**, 13041–13048 (2000).
36. Liu, L.F., Liu, C.C. & Alberts, B.M. Type II DNA topoisomerases: enzymes that can unknot a topologically knotted DNA molecule via a reversible double-strand break. *Cell* **19**, 697–707 (1980).
37. Marini, J.C., Miller, K.G. & Englund, P.T. Decatenation of kinetoplast DNA by topoisomerases. *J. Biol. Chem.* **255**, 4976–4979 (1980).
38. Osheroff, N. & Zechiedrich, E.L. Calcium-promoted DNA cleavage by eukaryotic topoisomerase II: trapping the covalent enzyme-DNA complex in an active form. *Biochemistry* **26**, 4303–4309 (1987).
39. Lindsley, J.E. Use of a real-time, coupled assay to measure the ATPase activity of DNA topoisomerase II. *Methods Mol. Biol.* **95**, 57–64 (2001).
40. Tamura, J.K. & Gellert, M. Characterization of the ATP binding site on *Escherichia coli* DNA gyrase. Affinity labeling of Lys-103 and Lys-110 of the B subunit by pyridoxal 5′-diphospho-5′-adenosine. *J. Biol. Chem.* **265**, 21342–21349 (1990).
41. Maxwell, A. & Gellert, M. The DNA dependence of the ATPase activity of DNA gyrase. *J. Biol. Chem.* **259**, 14472–14480 (1984).
42. Hammonds, T.R. & Maxwell, A. The DNA dependence of the ATPase activity of human DNA topoisomerase IIα. *J. Biol. Chem.* **272**, 32696–32703 (1997).
43. West, K.L., Turnbull, R.M., Willmore, E., Lakey, J.H. & Austin, C.A. Characterisation of the DNA-dependent ATPase activity of human DNA topoisomerase IIbeta: mutation of Ser165 in the ATPase domain reduces the ATPase activity and abolishes the *in vivo* complementation ability. *Nucleic Acids Res.* **30**, 5416–5424 (2002).
44. Mueller-Planitz, F. & Herschlag, D. DNA topoisomerase II selects DNA cleavage sites based on reactivity rather than binding affinity. *Nucleic Acids Res.* **35**, 3764–3773 (2007).
45. Shiozaki, K. & Yanagida, M. Functional dissection of the phosphorylated termini of fission yeast DNA topoisomerase II. *J. Cell Biol.* **119**, 1023–1036 (1992).
46. Cardenas, M.E., Dang, Q., Glover, C.V. & Gasser, S.M. Casein kinase II phosphorylates the eukaryote-specific C-terminal domain of topoisomerase II *in vivo*. *EMBO J.* **11**, 1785–1796 (1992).
47. McClendon, A.K. *et al.* Bimodal recognition of DNA geometry by human topoisomerase II α: preferential relaxation of positively supercoiled DNA requires elements in the C-terminal domain. *Biochemistry* **47**, 13169–13178 (2008).
48. Caron, P.R., Watt, P. & Wang, J.C. The C-terminal domain of *Saccharomyces cerevisiae* DNA topoisomerase II. *Mol. Cell. Biol.* **14**, 3197–3207 (1994).
49. Roca, J. The path of the DNA along the dimer interface of topoisomerase II. *J. Biol. Chem.* **279**, 25783–25788 (2004).
50. Baird, C.L., Harkins, T.T., Morris, S.K. & Lindsley, J.E. Topoisomerase II drives DNA transport by hydrolyzing one ATP. *Proc. Natl. Acad. Sci. USA* **96**, 13685–13690 (1999).
51. Osheroff, N. Eukaryotic topoisomerase II. Characterization of enzyme turnover. *J. Biol. Chem.* **261**, 9944–9950 (1986).
52. Tingey, A.P. & Maxwell, A. Probing the role of the ATP-operated clamp in the strand-passage reaction of DNA gyrase. *Nucleic Acids Res.* **24**, 4868–4873 (1996).
53. Li, W. & Wang, J.C. Footprinting of yeast DNA topoisomerase II lysyl side chains involved in substrate binding and interdomainal interactions. *J. Biol. Chem.* **272**, 31190–31195 (1997).
54. Choudhary, C. *et al.* Lysine acetylation targets protein complexes and co-regulates major cellular functions. *Science* **325**, 834–840 (2009).
55. Bates, A.D., Berger, J.M. & Maxwell, A. The ancestral role of ATP hydrolysis in type II topoisomerases: prevention of DNA double-strand breaks. *Nucleic Acids Res.* **39**, 6327–6339 (2011).
56. Ali, M.M. *et al.* Crystal structure of an Hsp90-nucleotide-p23/Sba1 closed chaperone complex. *Nature* **440**, 1013–1017 (2006).
57. Gellert, M., Mizuuchi, K., O'Dea, M.H. & Nash, H.A. DNA gyrase: an enzyme that introduces superhelical turns into DNA. *Proc. Natl. Acad. Sci. USA* **73**, 3872–3876 (1976).
58. Lee, S. *et al.* DNA cleavage and opening reactions of human topoisomerase IIα are regulated via Mg^{2+}-mediated dynamic bending of gate-DNA. *Proc. Natl. Acad. Sci. USA* **109**, 2925–2930 (2012).
59. Skouboe, C. *et al.* A human topoisomerase II α heterodimer with only one ATP binding site can go through successive catalytic cycles. *J. Biol. Chem.* **278**, 5768–5774 (2003).
60. Göttler, T. & Klostermeier, D. Dissection of the nucleotide cycle of *B. subtilis* DNA gyrase and its modulation by DNA. *J. Mol. Biol.* **367**, 1392–1404 (2007).

ONLINE METHODS

Topo II expression and purification. Residues 1–1,177 of *S. cerevisiae* topoisomerase II were expressed as a fusion with an amino-terminal tobacco etch virus (TEV) protease–cleavable hexahistidine (His_6) tag. Prior studies have shown that this construct retains the full catalytic activity of the wild-type protein *in vitro* but lacks nuclear-localization elements that would allow it to complement a *top2* ts allele *in vivo*[48]. Overexpression was carried out in *S. cerevisiae* strain BCY123 grown in complete supplement mixture dropout medium lacking uracil (CSM-URA), supplemented with lactic acid (2%) and glycerol (1.5%) for a carbon source. Galactose (20 g l^{-1}) was added, when cultures reached an OD of 0.8, for induction (6 h at 30 °C). Induced cells were collected by centrifugation, resuspended in Buffer A (300 mM KCl, 20 mM Tris-HCl, pH 8.5, 10% glycerol, 20 mM imidazole, pH 8.0, 1 mM phenylmethylsulfonyl fluoride), flash frozen in liquid nitrogen and lysed by grinding under liquid nitrogen. Ground cell powder was resuspended in Buffer A and centrifuged (20 min, 16,000 r.p.m.) to clarify the lysate. Protein was purified by tandem nickel-affinity and ion-exchange chromatography (nickel-chelating Sepharose and HiTrap SP, GE) followed by removal of the His_6 tag with His_6-tagged TEV protease and passage over a second nickel-affinity column to remove uncleaved protein and the protease. The protein was then run over a gel-filtration column (S-300, GE) equilibrated in 10% glycerol, 500 mM KCl and 20 mM Tris, pH 7.9. Peak fractions were assessed by SDS-PAGE, collected and concentrated in Amicon 100-kDa–cutoff concentrators (Millipore).

Human topo IIα was prepared similarly to the yeast enzyme but was not tagged with a hexahistidine tag. As such, after resuspension in Buffer A (without imidazole), a 35% ammonium sulfate precipitation step followed by centrifugation was performed. The resultant supernatant, which contains topo IIα, was subjected to an additional 65% ammonium sulfate cut, after which the protein was spun down in the precipitate. The precipitated protein was resuspended in 100 mM KCl, 20 mM Tris-HCl, pH 8.5, 10% glycerol, 1 mM phenylmethylsulfonyl fluoride and flowed over an ion-exchange column (HiTrap SP, GE). The protein was eluted with an increasing KCl salt gradient and then collected and run over a gel-filtration column (S-300, GE) equilibrated in 10% glycerol, 500 mM KCl and 20 mM Tris-Cl, pH 7.9. Peak fractions were assessed by SDS-PAGE, collected, and concentrated in Amicon 100-kDa–cutoff concentrators (Millipore).

Covalent-complex formation and purification. Both standard and phosphorothiolate oligonucleotides were synthesized on an in-house ABI synthesizer. Phosphorothioamidite for producing the 3′-bridging phosphorothiolate was synthesized as reported[61]. After synthesis, DNAs were purified by running on a denaturing urea-formamide 12% polyacrylamide gel, illuminating by UV, excising the bands, crushing the gel matrix and eluting overnight into 500 mM ammonium acetate and 10 mM magnesium acetate. The oligonucleotides were then cleaned with a C18 column (Waters), lyophilized overnight and resuspended in 10 mM Tris-Cl, pH 7.9 and 200 mM KCl. The oligonucleotide containing the phosphorothiolated bond was mixed with the two shorter oligonucleotides to assemble a singly nicked substrate (**Supplementary Fig. 1**), heated to 90 °C in a water bath and cooled to room temperature overnight to anneal. For production of the cleavage complex, annealed oligonucleotides were incubated for 45 min at room temperature at a 1.2:1 molar ratio of oligonucleotide:enzyme in 100 mM KCl, 10 mM Tris, pH 7.9, 5 mM $MnCl_2$ and 1 mM AMPPNP. Unreacted protein, DNA and nucleotide were separated from the complex by passing the sample over a gel-filtration column (S-300, GE) and cation-exchange column (HiTrap SP, GE) connected in series and pre-equilibrated with 20 mM Tris, pH 7.9, 100 mM KCl and 5 mM $MgCl_2$. The gel-filtration column removed unbound DNA from the protein, whereas unbound protein and the DNA-cleavage complex were separated by the cation-exchange column. The protein–DNA complex was then concentrated to 5 mg ml^{-1} in the column buffer with fresh AMPPNP added to 1 mM final concentration.

Crystallization and structure solution. Crystals were grown at 18 °C in hanging-drop format by mixing 1 µl protein solution with 1 µl well solution containing 23% PEG 300 and 100 mM Tris, pH 8.0. For harvesting, crystals were transferred for one minute to well solution containing 10% xylitol and then looped and flash frozen in liquid nitrogen. Data were collected at Beamline 8.3.1 (wavelength 1.1159 Å) under a cryo-stream at the Advanced Light Source (ALS) at Lawrence Berkeley National Laboratory and integrated by using HKL2000 (ref. 62). Initial phases were calculated by molecular replacement (MR) using two independent search models for PHASER[63]. The first model corresponded to a single DNA-free promoter from the cleavage complex of the *S. cerevisiae* topo II DNA-binding-and-cleavage core (residues 421–1,177 of PDB ID 3L4J)[27] and the second to one protomer from the *S. cerevisiae* topo II ATPase domain dimer (residues 7–406 of PDB ID 1PVG)[17]. The final MR solution regenerated one intact holoenzyme dimer in the asymmetric unit and resulted in clear electron density for the duplex DNA substrate in difference maps. Building of the model was carried out in COOT[64], followed by a refinement strategy using PHENIX[65] that consisted of an initial round of rigid-body refinement, followed only by individual-atom and TLS refinement. For individual atom refinement, both secondary-structure restraints and NCS restraints were employed, with refinement parameters weighted to highly favor geometry. This approach kept most side chain rotamers in their original conformers, improved the model's geometry, better placed the peptide backbone into electron density maps and markedly improved R_{free}. Structure validation was assisted by MolProbity[66], and figures were rendered by using PyMOL[67]. As calculated by MolProbity, 97.7% of main chain torsion angles fell within favored regions of Ramachandran space, with only 2.3% in allowed regions and 0% in disallowed.

Notes on structure modeling. Because a nonpalindromic DNA sequence was used for co-crystallization (**Supplementary Fig. 1**), electron density for the DNA corresponded to an average of the two possible sequence orientations. To account for this overlap, we modeled the DNA density as two alternate oligonucleotide segments, each present at half occupancy. We note that such an approach has been used in similar circumstances[27] and that the DNA-sequence orientation does not alter any subsequent analysis or conclusions in this paper.

DNA supercoiling-relaxation, decatenation and cleavage assays. Wild-type or mutant topo II (or topo IIα) was incubated with 300 ng (7.5 µM) of negatively supercoiled pUC19 plasmid DNA or kDNA in 20 µL reactions for 30 min at either 30 °C (for the yeast enzyme) or 37 °C (human protein). The final reaction conditions included 10 mM Tris, pH 7.9, 100 mM KCl, 5 mM $MgCl_2$, 2% glycerol and 1 mM ATP. Reactions were stopped with the addition of 0.5% SDS and 12.5 mM EDTA (final concentrations) and then treated with proteinase K for 30 min at 42 °C. Sucrose-based loading dye was added to samples, and samples were run on a 1.2% agarose (Invitrogen), 1X TAE gel at 1–1.5 V cm^{-1} for 16–18 h. Gels were stained with 0.5 µg ml^{-1} ethidium bromide (EtBr) for 20 min, followed by destaining for 30 min. Bands were visualized by UV transillumination.

ATPase assay. Wild-type and mutant topo II ATPase activities were measured by using an established enzyme-coupled assay in which the hydrolysis of ATP to ADP is coupled to the oxidation of NADH to NAD^+ (refs. 39,40). To determine standard kinetic parameters (K_m, V_{max}), we incubated 50 nM homodimeric enzyme with 0–4 mM ATP in 75-µl reactions. Reactions contained 50 mM Tris, pH 7.9, 100 mM KCl, 8 mM $MgCl_2$, 5 mM β-mercaptoethanol, 0.2 mg ml^{-1} bovine serum albumin, 2 mM phosphoenol pyruvate (PEP), 0.2 mM β-nicotinamide adenine dinucleotide (NADH), and an excess of pyruvate kinase and lactate dehydrogenase (enzyme mix obtained from Sigma). Assays were performed at 30 °C for yeast and 37 °C for human enzymes, with the oxidation of NADH to NAD^+ monitored by measuring absorbance at 340 nm in a PerkinElmer Victor ^{3}V 1420 multilabel plate reader. The rate of decrease in absorbance was converted to µmol of ATP hydrolyzed to ADP by using an NADH standard curve and the assumption that one ATP is hydrolyzed for every NADH oxidized. ATPase rate as a function of ATP concentration was fit for K_m and V_{max} by using Michaelis-Menten kinetics in KaleidaGraph (Synergy Software). DNA stimulation of ATPase activity was measured by using assays performed as described, except that the starting concentration of ATP was held constant (0.25 mM for yeast and 1 mM for human), and reactions were supplemented either with varying amounts of purified sheared salmon-sperm DNA (Sigma) or with oligonucleotide substrates (IDT); in analyzing ATPase activity measured as a function of salmon sperm DNA concentration, use of the Hill equation resulted in a much better fit to the observed data than did Michaelis-Menten treatment. In experiments of oligonucleotide-stimulated ATPase rates, oligonucleotides were titrated up to 12.5 µM, a 250:1 molar ratio of oligonucleotide:enzyme, where the stimulative effect of DNA was at a maximum.

61. Deweese, J.E., Burgin, A.B. & Osheroff, N. Using 3′-bridging phosphorothiolates to isolate the forward DNA cleavage reaction of human topoisomerase IIα. *Biochemistry* **47**, 4129–4140 (2008).
62. Otwinowski, Z. & Minor, W. Processing of X-ray diffraction data collected in oscillation mode. *Methods Enzymol.* **276**, 307–326 (1997).
63. McCoy, A.J. *et al.* Phaser crystallographic software. *J. Appl. Crystallogr.* **40**, 658–674 (2007).
64. Emsley, P., Lohkamp, B., Scott, W.G. & Cowtan, K. Features and development of Coot. *Acta Crystallogr. D Biol. Crystallogr.* **66**, 486–501 (2010).
65. Adams, P.D. *et al.* PHENIX: a comprehensive Python-based system for macromolecular structure solution. *Acta Crystallogr. D Biol. Crystallogr.* **66**, 213–221 (2010).
66. Chen, V.B. *et al.* MolProbity: all-atom structure validation for macromolecular crystallography. *Acta Crystallogr. D Biol. Crystallogr.* **66**, 12–21 (2010).
67. The PyMOL Molecular Graphics System. Version 1.5.0.1 Schrödinger, LLC.

 doi:10.1038/nsmb.2388